

## EMBEDDED MINIMAL DISKS: PROPER VERSUS NONPROPER—GLOBAL VERSUS LOCAL

TOBIAS H. COLDING AND WILLIAM P. MINICOZZI II

ABSTRACT. We construct a sequence of compact embedded minimal disks in a ball in  $\mathbf{R}^3$  with boundaries in the boundary of the ball and where the curvatures blow up only at the center. The sequence converges to a limit which is not smooth and not proper. If instead the sequence of embedded disks had boundaries in a sequence of balls with radii tending to infinity, then we have shown previously that any limit must be smooth and proper.

### 0. INTRODUCTION

Consider a sequence of compact embedded minimal disks  $\Sigma_i \subset B_{R_i} = B_{R_i}(0) \subset \mathbf{R}^3$  with  $\partial\Sigma_i \subset \partial B_{R_i}$  and either

- (a)  $R_i$  equal to a finite constant, or
- (b)  $R_i \rightarrow \infty$ .

We will refer to (a) as the *local case* and to (b) as the *global case*. Recall that a surface  $\Sigma \subset \mathbf{R}^3$  is said to be properly embedded if it is embedded and the intersection of  $\Sigma$  with any compact subset of  $\mathbf{R}^3$  is compact. We say that a lamination or foliation is proper if each leaf is proper.

We will be interested in the possible limits of sequences of minimal disks  $\Sigma_i$  as above where the curvatures blow up, e.g.,  $\sup_{B_1 \cap \Sigma_i} |A|^2 \rightarrow \infty$  as  $i \rightarrow \infty$ . In the global case, Theorem 0.1 in [CM2] gives a subsequence converging off a Lipschitz curve to a foliation by parallel planes; cf. Figure 1. In particular, the limit is a (smooth) foliation which is proper. We show here in Theorem 1 that smoothness and properness of the limit can fail in the local case; cf. Figure 2.

We will need the notion of a multi-valued graph; see Figure 3. Let  $D_r \subset \mathbf{C}$  be the disk in the plane centered at the origin and of radius  $r$ , and let  $\mathcal{P}$  be the universal cover of the punctured plane  $\mathbf{C} \setminus \{0\}$  with global polar coordinates  $(\rho, \theta)$  so  $\rho > 0$  and  $\theta \in \mathbf{R}$ . An  $N$ -valued graph on the annulus  $D_s \setminus D_r$  is a single valued graph of a function  $u$  over  $\{(\rho, \theta) \mid r < \rho \leq s, |\theta| \leq N\pi\}$ .

In Theorem 1, we construct a sequence of disks  $\Sigma_i \subset B_1 = B_1(0) \subset \mathbf{R}^3$  as above where the curvatures blow up only at 0 (see (1) and (2)) and  $\Sigma_i \setminus \{x_3\text{-axis}\}$  consists of two multi-valued graphs for each  $i$ ; see (3). Furthermore (see (4)),  $\Sigma_i \setminus \{x_3 = 0\}$  converges to two embedded minimal disks  $\Sigma^- \subset \{x_3 < 0\}$  and  $\Sigma^+ \subset \{x_3 > 0\}$ , each of which spirals into  $\{x_3 = 0\}$  and thus is not proper; see Figure 2.

---

Received by the editors October 21, 2002.

2000 *Mathematics Subject Classification*. Primary 53A10, 49Q05.

The authors were partially supported by NSF Grants DMS 0104453 and DMS 0104187.

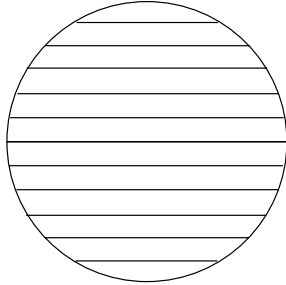


FIGURE 1. The limit in a ball of a sequence of degenerating helicoids is a foliation by parallel planes. This is smooth and proper.

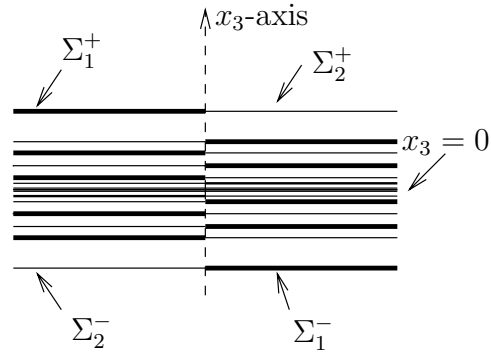


FIGURE 2. A schematic picture of the limit in Theorem 1 which is not smooth and not proper (the dotted  $x_3$ -axis is part of the limit). The limit contains four multi-valued graphs joined at the  $x_3$ -axis;  $\Sigma_1^+, \Sigma_2^+$  above the plane  $x_3 = 0$  and  $\Sigma_1^-, \Sigma_2^-$  below the plane. Each of the four spirals into the plane.

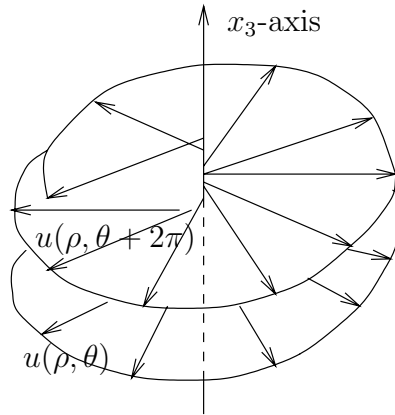


FIGURE 3. A multi-valued graph of a function  $u$ .

**Theorem 1.** *There is a sequence of compact embedded minimal disks  $0 \in \Sigma_i \subset B_1 \subset \mathbf{R}^3$  with  $\partial \Sigma_i \subset \partial B_1$  and containing the vertical segment  $\{(0, 0, t) \mid |t| < 1\} \subset \Sigma_i$ , and such that the following conditions are satisfied:*

- (1)  $\lim_{i \rightarrow \infty} |A_{\Sigma_i}|^2(0) = \infty$ .
- (2)  $\sup_i \sup_{\Sigma_i \setminus B_\delta} |A_{\Sigma_i}|^2 < \infty$  for all  $\delta > 0$ .
- (3)  $\Sigma_i \setminus \{x_3\text{-axis}\} = \Sigma_{1,i} \cup \Sigma_{2,i}$  for multi-valued graphs  $\Sigma_{1,i}$  and  $\Sigma_{2,i}$ .
- (4)  $\Sigma_i \setminus \{x_3 = 0\}$  converges to two embedded minimal disks  $\Sigma^\pm \subset \{\pm x_3 > 0\}$  with  $\overline{\Sigma^\pm} \setminus \Sigma^\pm = B_1 \cap \{x_3 = 0\}$ . Moreover,  $\Sigma^\pm \setminus \{x_3\text{-axis}\} = \Sigma_1^\pm \cup \Sigma_2^\pm$  for multi-valued graphs  $\Sigma_1^\pm$  and  $\Sigma_2^\pm$  each of which spirals into  $\{x_3 = 0\}$ ; see Figure 2.

It follows from (4) that  $\Sigma_i \setminus \{0\}$  converges to a lamination of  $B_1 \setminus \{0\}$  (with leaves  $\Sigma^-, \Sigma^+$ , and  $B_1 \cap \{x_3 = 0\} \setminus \{0\}$ ) which does not extend to a lamination of  $B_1$ . Namely, 0 is not a removable singularity.

The multi-valued graphs that we will consider will never close up; in fact they will all be embedded. The most important example of an embedded minimal multi-valued graph comes from the helicoid. The *helicoid* is the minimal surface  $\Sigma$  in  $\mathbf{R}^3$  parametrized by  $(s \cos t, s \sin t, t)$ , where  $s, t \in \mathbf{R}$ . Thus  $\Sigma \setminus \{x_3\text{-axis}\} = \Sigma_1 \cup \Sigma_2$ , where  $\Sigma_1, \Sigma_2$  are  $\infty$ -valued graphs on  $\mathbf{C} \setminus \{0\}$ .  $\Sigma_1$  is the graph of the function  $u_1(\rho, \theta) = \theta$  and  $\Sigma_2$  is the graph of the function  $u_2(\rho, \theta) = \theta + \pi$ .

We will use standard  $(x_1, x_2, x_3)$  coordinates on  $\mathbf{R}^3$  and  $z = x + iy$  on  $\mathbf{C}$ . Given  $f : \mathbf{C} \rightarrow \mathbf{C}^n$ ,  $\partial_x f$  and  $\partial_y f$  denote  $\frac{\partial f}{\partial x}$  and  $\frac{\partial f}{\partial y}$ , respectively; similarly,  $\partial_z f = (\partial_x f - i\partial_y f)/2$ . For  $p \in \mathbf{R}^3$  and  $s > 0$ , the ball in  $\mathbf{R}^3$  is  $B_s(p)$ .  $K_\Sigma$  is the sectional curvature of a smooth surface  $\Sigma$ . When  $\Sigma$  is immersed in  $\mathbf{R}^3$ , then  $A_\Sigma$  will be its second fundamental form (so when  $\Sigma$  is minimal, then  $|A_\Sigma|^2 = -2K_\Sigma$ ). When  $\Sigma$  is oriented,  $\mathbf{n}_\Sigma$  is the unit normal.

## 1. PRELIMINARIES ON THE WEIERSTRASS REPRESENTATION

Let  $\Omega \subset \mathbf{C}$  be a domain. The classical Weierstrass representation (see [Os]) starts from a meromorphic function  $g$  on  $\Omega$  and a holomorphic one-form  $\phi$  on  $\Omega$ , and associates to them a (branched) conformal minimal immersion  $F : \Omega \rightarrow \mathbf{R}^3$  by

$$(1.1) \quad F(z) = \operatorname{Re} \int_{\zeta \in \gamma_{z_0, z}} \left( \frac{1}{2} (g^{-1}(\zeta) - g(\zeta)), \frac{i}{2} (g^{-1}(\zeta) + g(\zeta)), 1 \right) \phi(\zeta).$$

Here  $z_0 \in \Omega$  is a fixed base point and the integration is along a path  $\gamma_{z_0, z}$  from  $z_0$  to  $z$ . The choice of  $z_0$  changes  $F$  by adding a constant. We will assume that  $F(z)$  does not depend on the choice of path  $\gamma_{z_0, z}$ ; this is the case, for example, when  $g$  has no zeros or poles and  $\Omega$  is simply connected.

The unit normal  $\mathbf{n}$  and Gauss curvature  $K$  of the resulting surface are then (see sections 8, 9 in [Os])

$$(1.2) \quad \mathbf{n} = (2 \operatorname{Re} g, 2 \operatorname{Im} g, |g|^2 - 1) / (|g|^2 + 1),$$

$$(1.3) \quad K = - \left[ \frac{4|\partial_z g| |g|}{|\phi| (1 + |g|^2)^2} \right]^2.$$

Since the pullback  $F^*(dx_3)$  is  $\operatorname{Re} \phi$  by (1.1),  $\phi$  is usually called the *height differential*. By (1.2),  $g$  is the composition of the Gauss map followed by stereographic projection.

To ensure that  $F$  is an immersion (i.e.,  $dF \neq 0$ ), we will assume that  $\phi$  does not vanish and  $g$  has no zeros or poles. The two standard examples are

$$(1.4) \quad g(z) = z, \phi(z) = dz/z, \Omega = \mathbf{C} \setminus \{0\}, \text{ giving a catenoid,}$$

$$(1.5) \quad g(z) = e^{iz}, \phi(z) = dz, \Omega = \mathbf{C}, \text{ giving a helicoid.}$$

The next lemma records the differential of  $F$ .

**Lemma 1.** *If  $F$  is given by (1.1) with  $g(z) = e^{i(u(z)+iv(z))}$  and  $\phi = dz$ , then*

$$(1.6) \quad \partial_x F = (\sinh v \cos u, \sinh v \sin u, 1),$$

$$(1.7) \quad \partial_y F = (\cosh v \sin u, -\cosh v \cos u, 0).$$

2. THE PROOF OF THEOREM 1

To show Theorem 1, we first construct a one-parameter family (with parameter  $a \in (0, 1/2)$ ) of minimal immersions  $F_a$  by making a specific choice of Weierstrass data  $g = e^{ih_a}$  (where  $h_a = u_a + i v_a$ ),  $\phi = dz$ , and domain  $\Omega_a$  to use in (1.1). We show in Lemma 2 that this one-parameter family of immersions is compact. Lemma 3 shows that the immersions  $F_a : \Omega_a \rightarrow \mathbf{R}^3$  are embeddings.

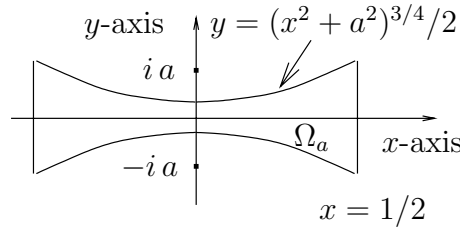


FIGURE 4. The domain  $\Omega_a$ .

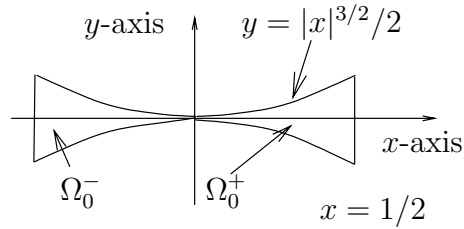


FIGURE 5.  $\Omega_0 = \bigcap_{a>0} \Omega_a \setminus \{0\}$  and its two components  $\Omega_0^+$  and  $\Omega_0^-$ .

For each  $0 < a < 1/2$ , set (see Figure 4)

$$(2.1) \quad h_a(z) = \frac{1}{a} \arctan\left(\frac{z}{a}\right) \text{ on } \Omega_a = \{(x, y) \mid |x| \leq 1/2, |y| \leq (x^2 + a^2)^{3/4}/2\}.$$

Note that  $h_a$  is well-defined, since  $\Omega_a$  is simply connected and  $\pm ia \notin \Omega_a$ . For future reference,

$$(2.2) \quad \partial_z h_a(z) = \frac{1}{z^2 + a^2} = \frac{x^2 + a^2 - y^2 - 2i xy}{(x^2 + a^2 - y^2)^2 + 4x^2 y^2},$$

$$(2.3) \quad K_a(z) = \frac{-|\partial_z h_a|^2}{\cosh^4 v_a} = \frac{-|z^2 + a^2|^{-2}}{\cosh^4(\text{Im } \arctan(z/a)/a)}.$$

Here (2.3) used (1.3). Note that, by the Cauchy-Riemann equations,

$$(2.4) \quad \partial_z h_a = (\partial_x - i \partial_y)(u_a + i v_a)/2 = \partial_x u_a - i \partial_y u_a = \partial_y v_a + i \partial_x v_a.$$

In the rest of this paper we let  $F_a : \Omega_a \rightarrow \mathbf{R}^3$  be from (1.1) with  $g = e^{ih_a}$ ,  $\phi = dz$ , and  $z_0 = 0$ . Set  $\Omega_0 = \bigcap_a \Omega_a \setminus \{0\}$ , so  $\Omega_0 = \{(x, y) \mid 0 < |x| \leq 1/2, |y| \leq |x|^{3/2}/2\}$ ; see Figure 5. The family of functions  $h_a$  is not compact, since  $\lim_{a \rightarrow 0} |h_a|(z) = \infty$  for  $z \in \Omega_0$ . However, the next lemma shows that the family of immersions  $F_a$  is compact.

**Lemma 2.** *If  $a_j \rightarrow 0$ , then there is a subsequence  $a_i$  for which  $F_{a_i}$  converges uniformly in  $C^2$  on compact subsets of  $\Omega_0$ .*

*Proof.* Since  $h_a$  and  $-1/z$  are holomorphic and

$$(2.5) \quad |\partial_z h_a(z) - \partial_z(-1/z)| = a^2 |z|^{-2} |z^2 + a^2|^{-1},$$

we get easily that  $\nabla h_a$  converges as  $a \rightarrow 0$  to  $\nabla(-1/z)$  uniformly on compact subsets of  $\Omega_0$ . Since each  $v_a(x, 0) = 0$ , the fundamental theorem of calculus gives that the  $v_a$ 's converge uniformly in  $C^1$  on compact subsets of  $\Omega_0$ . (Unfortunately, the  $u_a$ 's do not converge.)

Let  $\Omega_0^\pm = \{\pm x > 0\} \cap \Omega_0$  be the two components of  $\Omega_0$ ; see Figure 5. Set  $b_j^+ = u_{a_j}(1/2)$  and  $b_j^- = u_{a_j}(-1/2)$  and choose a subsequence  $a_i$  so both  $b_i^-$  and  $b_i^+$

converge modulo  $2\pi$  (this is possible since  $T^2 = \mathbf{R}^2/(2\pi\mathbf{Z}^2)$  is compact). Arguing as above, we find that  $h_{a_i} - b_i^\pm$  converges uniformly in  $C^1$  on compact subsets of  $\Omega_0^\pm$ . Therefore, by Lemma 1, the minimal immersions corresponding to Weierstrass data  $g = e^{i(h_{a_i} - b_i^\pm)}$ ,  $\phi = dz$  converge uniformly in  $C^2$  on compact subsets of  $\Omega_0^\pm$  as  $i \rightarrow \infty$ .  $\square$

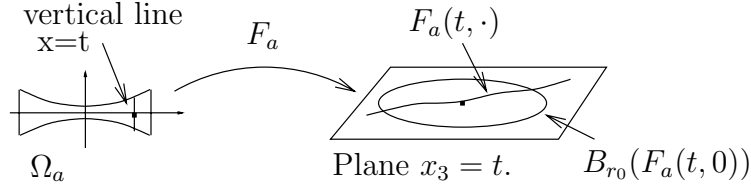


FIGURE 6. A horizontal slice in Lemma 3.

The main difficulty in proving Theorem 1 is showing that the immersions  $F_a : \Omega_a \rightarrow \mathbf{R}^3$  are embeddings. This will follow easily from (A) and (B) below. Namely, we show in Lemma 3, see Figures 6 and 7, that for  $|t| \leq 1/2$ :

(A) The horizontal slice  $\{x_3 = t\} \cap F_a(\Omega_a)$  is the image of the vertical segment  $\{x = t\}$  in the plane, i.e.,  $x_3(F_a(x, y)) = x$ ; see (2.6).

(B) The image  $F_a(\{x = t\} \cap \Omega_a)$  is a graph over a line segment in the plane  $\{x_3 = t\}$  (the line segment will depend on  $t$ ); see (2.7).

(C) The boundary of the graph in (B) is outside the ball  $B_{r_0}(F_a(t, 0))$  for some  $r_0 > 0$  and all  $a$ ; see (2.8).

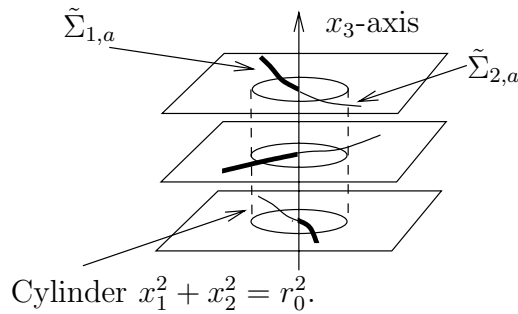


FIGURE 7. Horizontal slices of  $F_a(\Omega_a)$  in Lemma 3.

**Lemma 3.**

$$(2.6) \quad x_3(F_a(x, y)) = x.$$

$$(2.7) \quad \begin{aligned} \text{The curve } F_a(x, \cdot) : & [-(x^2 + a^2)^{3/4}/2, (x^2 + a^2)^{3/4}/2] \\ & \rightarrow \{x_3 = x\} \text{ is a graph.} \end{aligned}$$

$$(2.8) \quad |F_a(x, \pm(x^2 + a^2)^{3/4}/2) - F_a(x, 0)| > r_0 \text{ for some } r_0 > 0 \text{ and all } a.$$

*Proof.* Since  $z_0 = 0$  and  $\phi = dz$ , we get (2.6) from (1.1). Using  $y^2 < (x^2 + a^2)/4$  on  $\Omega_a$ , (2.2) and (2.4) give

$$(2.9) \quad |\partial_y u_a(x, y)| = \frac{2|xy|}{(x^2 + a^2 - y^2)^2 + 4x^2y^2} \leq \frac{4|xy|}{(x^2 + a^2)^2},$$

$$(2.10) \quad \partial_y v_a(x, y) = \frac{x^2 + a^2 - y^2}{(x^2 + a^2 - y^2)^2 + 4x^2y^2} > \frac{3}{8(x^2 + a^2)}.$$

Set  $y_{x,a} = (x^2 + a^2)^{3/4}/2$ . Integrating (2.9) gives

$$(2.11) \quad \max_{|y| \leq y_{x,a}} |u_a(x, y) - u_a(x, 0)| \leq \int_0^{y_{x,a}} \frac{4|x|t}{(x^2 + a^2)^2} dt = \frac{|x|}{2(x^2 + a^2)^{1/2}} < 1.$$

Set  $\gamma_{x,a}(y) = F_a(x, y)$ . Since  $v_a(x, 0) = 0$  and  $\cos(1) > 1/2$ , combining (1.7) and (2.11) gives

$$(2.12) \quad \langle \gamma'_{x,a}(y), \gamma'_{x,a}(0) \rangle = \cosh v_a(x, y) \cos(u_a(x, y) - u_a(x, 0)) > \cosh v_a(x, y)/2.$$

Here  $\gamma'_{x,a}(y) = \partial_y F_a(x, y)$ . By (2.12), the angle between  $\gamma'_{x,a}(y)$  and  $\gamma'_{x,a}(0)$  is always less than  $\pi/2$ ; this gives (2.7). Since  $v_a(x, 0) = 0$ , integrating (2.10) gives

$$(2.13) \quad \min_{y_{x,a}/2 \leq |y| \leq y_{x,a}} |v_a(x, y)| \geq \int_0^{y_{x,a}/2} \frac{3 dt}{8(x^2 + a^2)} = \frac{3}{32(x^2 + a^2)^{1/4}}.$$

Integrating (2.12) and using (2.13) gives

$$(2.14) \quad \langle \gamma_{x,a}(y_{x,a}) - \gamma_{x,a}(0), \gamma'_{x,a}(0) \rangle > \frac{(x^2 + a^2)^{3/4}}{16} e^{(x^2 + a^2)^{-1/4}/11}.$$

Since  $\lim_{s \rightarrow 0} s^3 e^{s^{-1}/11} = \infty$ , (2.14) and its analog for  $\gamma_{x,a}(-y_{x,a})$  give (2.8). □

**Corollary 1.** *See Figure 7. Let  $r_0$  be given by (2.8).*

- (i)  $F_a$  is an embedding.
- (ii)  $F_a(t, 0) = (0, 0, t)$  for  $|t| < 1/2$ .
- (iii)  $\{0 < x_1^2 + x_2^2 < r_0^2\} \cap F_a(\Omega_a) = \tilde{\Sigma}_{1,a} \cup \tilde{\Sigma}_{2,a}$  for multi-valued graphs  $\tilde{\Sigma}_{1,a}, \tilde{\Sigma}_{2,a}$  over  $D_{r_0} \setminus \{0\}$ .

*Proof.* Equations (2.6) and (2.7) immediately give (i).

Since  $z_0 = 0$ ,  $F(0, 0) = (0, 0, 0)$ . Integrating (1.6) and using  $v_a(x, 0) = 0$  then gives (ii).

By (1.2),  $F_a$  is “vertical,” i.e.,  $\langle \mathbf{n}, (0, 0, 1) \rangle = 0$ , when  $|g_a| = 1$ . However,  $|g_a(x, y)| = 1$  exactly when  $y = 0$ , so that, by (ii), the image is graphical away from the  $x_3$ -axis. Combining this with (2.8) gives (iii). □

Corollary 1 constructs the embeddings  $F_a$  that will be used in Theorem 1, and shows property (3). To prove Theorem 1, we need therefore only show (1), (2), and (4).

*Proof of Theorem 1.* By scaling, it suffices to find a sequence  $\Sigma_i \subset B_R$  for some  $R > 0$ . Corollary 1 gives minimal embeddings  $F_a : \Omega_a \rightarrow \mathbf{R}^3$  with  $F_a(t, 0) = (0, 0, t)$  for  $|t| < 1/2$ , and so (3) holds for any  $R \leq r_0$ . Set  $R = \min\{r_0/2, 1/4\}$  and  $\Sigma_i = B_R \cap F_{a_i}(\Omega_{a_i})$ , where the sequence  $a_i$  is to be determined.

To get (1), simply note that, by (2.3),  $|K_a|(0) = a^{-4} \rightarrow \infty$  as  $a \rightarrow 0$ .

We next show (2). First, by (2.3),  $\sup_a \sup_{\{|x| \geq \delta\} \cap \Omega_a} |K_a| < \infty$  for all  $\delta > 0$ . Combined with (3) and Heinz’s curvature estimate for minimal graphs (i.e., 11.7 in [Os]), this gives (2).

To get (4), use Lemma 2 to choose  $a_i \rightarrow 0$  so the mappings  $F_{a_i}$  converge uniformly in  $C^2$  on compact subsets to  $F_0 : \Omega_0 \rightarrow \mathbf{R}^3$ . Hence, by Lemma 3,  $\Sigma_i \setminus \{x_3 = 0\}$  converges to two embedded minimal disks  $\Sigma^\pm \subset F_0(\Omega_0^\pm)$  with  $\Sigma^\pm \setminus \{x_3\text{-axis}\} = \Sigma_1^\pm \cup \Sigma_2^\pm$  for multi-valued graphs  $\Sigma_j^\pm$ . To complete the proof, we show that each graph  $\Sigma_j^\pm$  is  $\infty$ -valued (and, hence, spirals into  $\{x_3 = 0\}$ ). Note that, by (3) and (1.7), the level sets  $\{x_3 = x\} \cap \Sigma_j^\pm$  are graphs over the line in the direction

$$(2.15) \quad \lim_{a \rightarrow 0} (\sin u_a(x, 0), -\cos u_a(x, 0), 0).$$

Therefore, since an easy calculation gives, for  $0 < t < 1/4$ ,

$$(2.16) \quad \lim_{a \rightarrow 0} |u_a(t, 0) - u_a(2t, 0)| = 1/(2t),$$

we see that  $\{t < |x_3| < 2t\} \cap \Sigma_j^\pm$  contains an embedded  $N_t$ -valued graph, where  $N_t \approx 1/(4\pi t) \rightarrow \infty$  as  $t \rightarrow 0$ . It follows that  $\Sigma_j^\pm$  must spiral into  $\{x_3 = 0\}$ , completing (4).  $\square$

#### REFERENCES

- [CM1] T.H. Colding and W.P. Minicozzi II, Embedded minimal disks, To appear in The Proceedings of the Clay Mathematics Institute Summer School on the Global Theory of Minimal Surfaces. MSRI. math.DG/0206146.
- [CM2] ———, The space of embedded minimal surfaces of fixed genus in a 3-manifold IV; Locally simply connected, preprint, math.AP/0210119.
- [Os] R. Osserman, A survey of minimal surfaces, *Dover*, 2nd. edition (1986). MR **87j**:53012

COURANT INSTITUTE OF MATHEMATICAL SCIENCES, 251 MERCER STREET, NEW YORK, NEW YORK 10012 AND PRINCETON UNIVERSITY, FINE HALL, WASHINGTON RD., PRINCETON, NEW JERSEY 08544-1000

*E-mail address:* `colding@cims.nyu.edu`

DEPARTMENT OF MATHEMATICS, JOHNS HOPKINS UNIVERSITY, 3400 N. CHARLES ST., BALTIMORE, MARYLAND 21218

*E-mail address:* `minicozz@jhu.edu`